BBA - General Subjects 1867 (2023) 130470

Contents lists available at ScienceDirect

BBA - General Subjects

journal homepage: www.elsevier.com/locate/bbagen

The D647N mutation of FGFR1 induces ligand-independent receptor activation

Mattia Domenichini [a], Cosetta Ravelli [a], Michela Corsini [a], Silvia Codenotti [a], Elisa Moreschi [a], Anna Gogna [a], Davide Capoferri [a], Daniela Zizioli [a], Roberto Bresciani [a,b], Elisabetta Grillo [a,*], Stefania Mitola [a,*]

[a] Department of Molecular and Translational Medicine, University of Brescia, Brescia 25123, Italy
[b] Highly Specialized Laboratory, Diagnostic Department, ASST Spedali Civili of Brescia, Brescia, Italy

ARTICLE INFO

Keywords:
FGFR1
Oncogenic mutation
Tyrosine kinase inhibitor
ATP

ABSTRACT

The activation loop (A-loop) of kinases, a key regulatory region, is recurrently mutated in several kinase proteins in cancer resulting in dysregulated kinase activity and response to kinase inhibitors. FGFR1 receptor tyrosine kinase represents an important oncogene and therapeutic target for solid and hematological tumors. Here we investigate the biochemical and molecular effects of D647N mutation lying in the A-loop of FGFR1.

When expressed in normal and tumoral *in vitro* cell models, $FGFR1^{D647N}$ is phosphorylated also in the absence of ligands, and this is accompanied by the activation of intracellular signaling. The expression of $FGFR1^{D647N}$ significantly increases single and collective migration of cancer cells *in vitro* and *in vivo*, when compared to $FGFR1^{WT}$. $FGFR1^{D647N}$ expression exacerbates the aggressiveness of cancer cells, increasing their invasiveness *in vitro* and augmenting their pro-angiogenic capacity *in vivo*.

Remarkably, the D647N mutation significantly increases the sensitivity of FGFR1 to the ATP-competitive inhibitor Erdafitinib suggesting the possibility that this mutation could become a specific target for the development of new inhibitors.

Although further efforts are warranted for an exhaustive description of the activation mechanisms, for the identification of more specific inhibitors and for confirming the clinical significance of mutated $FGFR1^{D647N}$, overall our data demonstrate that the D647N substitution of FGFR1 is a novel pro-oncogenic activating mutation of the receptor that, when found in cancer patients, may anticipate good response to erdafitinib treatment.

1. Introduction

Fibroblast growth factor receptor 1 (FGFR1) is a receptor tyrosine kinase (RTK) involved in several physiological and pathological processes including cell survival, proliferation, invasion, and apoptosis [1].

FGFR1 is characterized by three N-terminal immunoglobulin (Ig)-like binding domains, a transmembrane domain, and an intracellular tyrosine kinase domain (TKD). Aberrant regulation of the FGF/FGFR axis is involved in the onset and progression of solid tumors and hematological malignancies, including lung cancer, melanoma and multiple myeloma. The FGF/FGFR axis is the third most frequently altered pathway in cancer, after TP53 and KRAS. Genetic alterations in the FGF/FGFR pathways [single nucleotide variants (SNVs), gene amplifications, or gene fusions] occur in about 7% of tumors. Among the FGFRs, FGFR1 accounts for most of the alterations (approx. 49%), and only 5% of patients present multiple aberrations [2].

Several different point mutations have been described in all four FGFRs, including the activating point mutations N546K and K656E of FGFR1 [3–5].

The substitution D647N was recently identified using a protein domain-based pan-cancer analysis in which the mutational landscape of several RTKs was analyzed simultaneously [6]. Such pan-cancer study highlighted that position 256 of the consensus sequence of the kinase domain (KD), is recurrently mutated in several cancers. In particular mutations D647N in FGFR1 [NM023110.3, FGFR1 variant 1] and substitution L861Q/R in EGFR were identified in primary lesions of lung adenocarcinoma, substitution R1051Q in VEGFR2 and D1061N in FLT4 were identified in skin cancers, respectively in cutaneous squamous cell

* Corresponding authors at: Department of Molecular and Translational Medicine, University of Brescia, Viale Europa 11, Brescia 25123, Italy.
E-mail addresses: elisabetta.grillo@unibs.it (E. Grillo), stefania.mitola@unibs.it (S. Mitola).

https://doi.org/10.1016/j.bbagen.2023.130470
Received 10 July 2023; Received in revised form 11 September 2023; Accepted 28 September 2023
Available online 29 September 2023

carcinoma and melanoma and, the corresponding mutation D650H was identified in FGFR2 in stomach adenocarcinoma samples [7]. As expected, the expression of FGFR1^{D647N} and of other corresponding mutations in position 256 of the KD of RTKs reduce the overall survival of oncological patients [18]. The domain-based analysis suggests that specific residues in the protein domain can similarly affect protein functions, thus we can transfer functional and clinical information from known variants to uncharacterized mutations helping clinicians in the choose of therapy.

Analyzing all proteins belonging to the PK_Tyr_Ser-Thr protein family (Pfam: PF07714), position 256 corresponds to the well-known BRAF V600E mutation, a well-known molecular target for specific kinase inhibitors. Residue 256 is located in the activation loop (A-loop), a large flexible loop in the active site of kinases, characterized by the conserved residues DFG and APE at the beginning and at the end of the loop, respectively. The A-loop regulates kinase activity by changing its conformation. For this reason, much effort has been directed to design allosteric kinase inhibitors that interfere with the kinase structure, stabilizing the inactive state and/or destabilizing its active conformation [8]. In addition, ATP competitive inhibitors [9] and tyrosine kinase inhibitors (TKi) acting both as allosteric and orthosteric effectors [10] have been developed. Recently we characterized the effects of the mutation in position 256 of the KD in VEGFR2^{R1051Q}. This alteration constitutively activates the receptor and enhances cell metabolism supporting cell proliferation and dissemination when expressed in cancer cells.

On these bases we were prompted to investigate whether the analogous mutation in FGFR1 has similar effects. To this goal, in the present study we characterized the effects of the substitution D647N of FGFR1. Functional analyses demonstrated that D647N mutation increases the activity of FGFR1 and its related biological processes. Also, FGFR1^{D647N} shows a higher sensitivity to the FDA-approved TKi erdafitinib. Thus, the results confirm that position 256 of the KD is a key regulating residue for KD activity and that the identification of mutations at this position in FGFR1 and in other kinases may become of clinical interest for the diagnosis and/or for choosing the therapeutic options.

2. Material and methods

2.1. Mutagenesis

The cDNA of wild-type human FGFR1 (NM_023110.3) was cloned into pEF-I-GFPGX vector (kindly provided by Dr. Chung [11]). D647N point mutation was introduced using the QuikChange Lightning Site-directed Mutagenesis Kit (Agilent Technologies, Santa Clara, CA, USA), to generate the pEF-I-GFPGX_hFGFR1^{D647N} plasmid. For the mutagenesis reaction, the following primers were used: forward 5′-GGCCTCGCACGGAACATTCACCACATCG-3′; reverse 5′-CGATGTGGTGAATGTTCCGTGCGAGGCC-3′.

2.2. Cell culture

Human Embryonic Kidney HEK-293 T cells were grown in Dulbecco's Modified Eagle's Medium (DMEM, Thermo Fisher Scientific Inc., Waltham, Massachusetts, USA) containing 10% fetal bovine serum (FBS) (Thermo Fisher Scientific), 2 mM L-glutamine and penicillin/streptomycin. Human breast adenocarcinoma cell line MCF7 (purchased from American Type Culture Collection - ATCC, Manassass, Virginia, USA) were grown in DMEM-F12 supplemented with 10% FCS and penicillin/streptomycin. Human melanoma A375 cells (purchased from American Type Culture Collection - ATCC) were grown in DMEM supplemented with 10% FBS and penicillin/streptomycin.

Cells were transiently transfected with pEF-I-GFPGX_hFGFR1^{WT} or pEF-I-GFPGX_hFGFR1^{D647N} plasmids using FuGENE® HD Transfection Reagent (Promega Italia, Milano, Italy) or polyethylenimine (PEI 25 K™; PolySciences, Warrington) according to manufacturer's instructions.

To reduce the results variability due to different receptor expressions, three different transient transfections were performed. Transfected cells were sub aliquoted and frozen. All the experiments were performed on each transfection.

When indicated, cells were stimulated with recombinant human FGF2 [12] or challenged with the Erdafitinib (MedChemExpress, Monmouth Junction, New Jersey, USA).

2.3. Western Blot assay

Cells were lysed in lysis buffer [50 mM Tris-HCl buffer (pH 7.4), 150 mM NaCl, 1% Triton X-100, 0,2% Brij, 1 mM Na_3VO_4, protease and phosphatase inhibitors (Merck KGaA, Darmstadt, Germania)]. Total lysates (10–40 μg) were separated by SDS-PAGE and probed with anti-pY653/Y654-FGFRs, anti-pY766-FGFR1, anti-FGFR1, anti-pY436-FRS2-α, anti-pS473-Akt, or anti-p44/42 ERK (ERK 1/2) purchased from Cell Signaling Technology (Danvers, Massachusetts, USA) in a Western blot. Chemiluminescent signal was acquired by ChemiDoc™ Imaging System (BioRad, Hercules, California, USA).

2.4. Kinase assay

The reaction rate of ATP consumption was measured by the ADP-Glo™ Kinase Assay (Promega) following manufacturer's instructions. PolyE4Y1 peptide was used as a substrate for kinase phosphorylation. The reaction was carried out with different ATP concentrations between 0 and 1 mM. The intensity of the bioluminescence signal was detected through the EnSight Multimode Plate Reader (PerkinElmer, Waltham, Massachusetts, USA) at 520 nm wavelength.

For ADP-Glo™ kinase assay, data were analyzed considering the reaction as a specific binding and calculating the kinetic Michaelis constant (Km) as parameter of ATP-receptor binding affinity [13].

2.5. Measurement of TKi sensitivity

Transfected HEK-293 T were treated for 30 min with increasing doses of the specific TK inhibitor Erdafitinib. Cells were then lysed as before, and total lysates were separated by SDS-PAGE. Densitometry was used to quantify the FGFR1 receptor phosphorylation. GraphPad Software Prism 6.0 (GraphPadSoftware, Inc., San Diego, CA, USA) was used for Erdafitinib IC50 determination, based on decrease in receptor phosphorylation, and each experiment was repeated at least three times.

2.6. Immunofluorescence

Cells seeded onto μ-Slide chambered coverslip (Ibidi, Fitchburg, Massachusetts, USA) were fixed in a 4% paraformaldehyde solution in PBS (PFA 4%) and stained with anti-FGFR1, or anti-eea1 (BD Biosciences, Franklin Lakes, New Jersey, USA) followed by incubation with AlexaFluo 594-conjugated and an AlexaFluo 647 -conjugated secondary antibodies. Samples were analyzed with a LSM880 confocal microscope equipped with Plan-Apochromat 63×/1.4 NA oil objectives (Carl Zeiss, Jena, Germany) objectives. Image analysis was carried out using the open-source ImageJ software (imagej.nih.gov).

2.7. Motility assays

For scratch assay, confluent monolayers were scratched with a 200 μL tip to obtain a 2 mm-wide wound and incubated in 2% or 10% FBS-containing growth medium. Wounded monolayers were photographed after 16 and 24 h and the newly covered area was measured by ImageJ software (https://imagej.nih.gov/ij/download.html).

Alternatively, single cell migration assay was performed in a Boyden chamber (AP48 micro chemotaxis chamber; Neuroprobe, Pleasanton, CA), using a 8-μm pore size PVP-free polycarbonate filter (Neuroprobe,

Gaithersburg, Maryland, USA) coated on both sides with gelatin (0.01%). DMEM 2% FBS was added in the lower compartment of the chamber, and 1.0 × 10^6 cells/mL suspended in DMEM supplemented with 2% FCS were seeded in the upper compartment. After 5 h of incubation at 37 °C, cells migrated to the lower side of the filter were stained with Diff-Quik reagent. Five random fields were counted for each triplicate sample.

For *in vivo* cell migration, 1,5 × 10^5 cells resuspended in 15 μL of DMEM 10% FBS were seeded in a plastic ring placed on the chicken embryo chorioallantoic membrane (CAM). Exploiting the green fluorescence of transfected cells, migration was recorded under the stereo zoom microscope (Axio Zoom V16, Carl Zeiss) and acquired every 30 min for 2 h. Euclidean distance was measured by ImageJ tool.

2.8. Scattering assay

Spheroids were prepared plating 1 × 10^3 cells/well in round bottom plates in DMEM 10% FBS added with 20% methylcellulose for 48 h. Spheroids were embedded in fibrin gel and incubated for 24 h. The scattering index (total area - spheroid area/spheroid perimeter) was obtained by ImageJ software.

2.9. Angiogenesis assay

Cells were embedded in an alginic acid drop at the concentration of 1x10^4cells/μL. Alginate-cell spheres were transferred on the CAM surface [14]. The presence of neovessels growing towards the implant were analyzed and counted under a stereomicroscope (AxioZoom V6.1, Carl Zeiss) 4 days after implantation.

2.10. Statistical analyses

Data were processed using the statistical package Prism6 (GraphPad Software). To highlight the statistical difference between two groups of samples, Student's *t*-test for unpaired data was used, with a significance level set at $P < 0.05$.

3. Results

3.1. FGFR1^{D647N} substitution supports ligand-independent receptor phosphorylation

As we mentioned above D647N mutation is in the ATP binding site, thus we evaluated whether it affects FGR1 affinity for ATP. In order to define the ATP dissociation constant (Kd), we expressed FGFR1^{WT} and FGFR1^{D647N} in HEK 293 T cells and assessed them for the activity of receptor in the presence of increasing doses of ATP from 0 to 1 mM. Results show a similar Kd for both receptors respectively of 80.67 μM for FGFR1^{WT} and 111.5 μM for FGFR1^{D647N} (Fig. 1). Fig. 1a shows the mean results of three different transfections normalized on the timing of the reaction. Although the ATP affinity, FGFR1^{D647N} is more phosphorylated compared to FGFR1^{WT} in the absence of ligand in all transfections (Fig. 1b). Of note in all transfections FGFR1^{D647N} receptor is more expressed than the wild type. Similarly, observations were described for other RTK mutants in position 256 [5]. All results were normalized on the total receptor level.

Then we evaluated the effects of the expression of FGFR1^{D647N} in human breast cancer lines MCF7. As anticipated, Tyr653/654 within the A-loop of the FGFR1^{D647N} are highly phosphorylated also in a tumoral condition in the absence of ligands. Similarly, the phosphorylation of the Tyr766, a known docking site for PLCγ [15], is enhanced in FGFR1^{D647N}. We verified these results also in a melanoma cell model A375 (supplementary Fig. 1). Of note, similarly to FGFR1^{WT}, FGFR1^{D647N} remains responsive to FGF2 stimulation, suggesting that the receptor is still far from its maximum phosphorylation level (Fig. 2a). To an increase FGFR1^{D647N} phosphorylation corresponds to the activation of downstream mediators including the fibroblast growth factor receptor substrate 2 (FRS2), and ERK ½ (Fig.2a). According to the internalization of phosphorylated RTKs, most of FGFR1^{D647N} is internalized as demonstrated by immunofluorescence analysis performed on MCF7-FGFR1^{WT} and MCF7-FGFR1^{D647N}. A statistically significant difference in co-localization of FGFR1 with the Early Endosome Antigen 1 (eea1) highlights a higher presence of mutated FGFR1 in early endosome vesicles compared to FGFR1^{WT} (Fig. 2b). Again, results are normalized on the expression level of the receptors.

3.2. The expression of FGFR1^{D647N} exacerbates the invasive phenotype in tumor cells

Aberrant activation of the FGF/FGFR1 axis could affect tumor development and metastasization, resulting in a worse prognosis [16]. On these bases, we assessed the biological effect of FGFR1^{D647N} on cancer cell migration. The expression of FGFR1^{D647N} increases the motility of A375 and MCF7 cells compared to the FGFR1^{WT}-expressing cells in a scratch assay. The increased motility was detected both in the basal medium (2% FBS) or growth medium (10% FBS) (Fig. 3a,b). Similarly, FGFR1^{D647N}-expressing A375 cells migrate faster compared to FGFR1^{WT}-expressing ones in a Boyden chamber migration assay (Fig. 3c).

To confirm *in vitro* findings, we measured the motility of A375-FGFR1^{WT} and A375-FGFR1^{D647N} cells when engrafted on the chicken embryo chorioallantoic membrane (CAM) (Fig. 3d). Cell migration was recorded by time-lapse video-microscopy for 3 h under a Zoom microscope following the fluorescence of transfected cells. The Euclidean migratory distance covered by cells was calculated by ImageJ tool. Again, under these experimental conditions the expression of

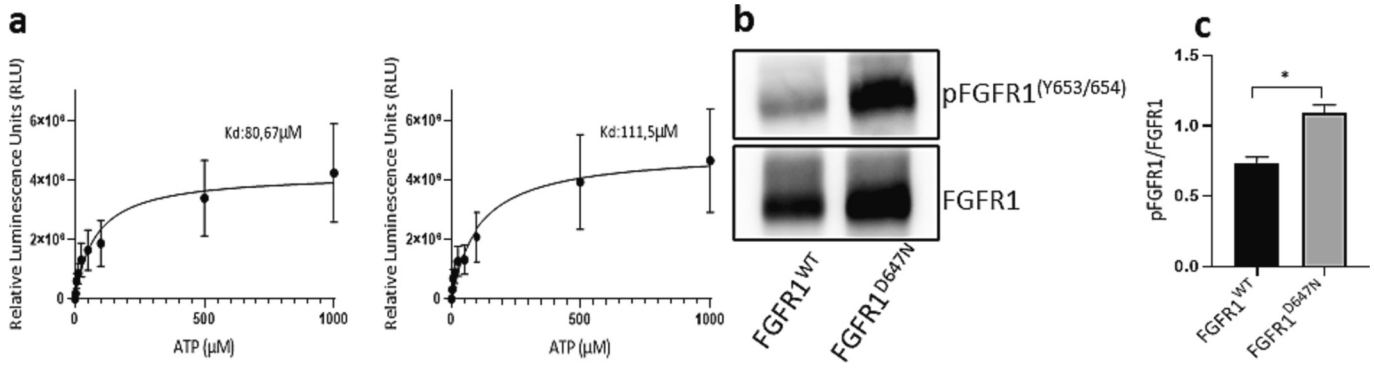

Fig. 1. FGFR1^{D647N} is phosphorylated in the absence of ligand. HEK 293 T cells were transfected with FGFR1^{WT} and FGFR1^{D647N}. a) ATP titration was measured for FGFR1^{WT} (left panel) and FGFR1^{D647N} (right panel); b) Phosphorylation of FGFR1^{WT} and FGFR1^{D647N} in the absence of ligand. c) Densitometric analysis of Western blot. Data are shown as the mean ± SD of 3 independent transfections performed in duplicate.

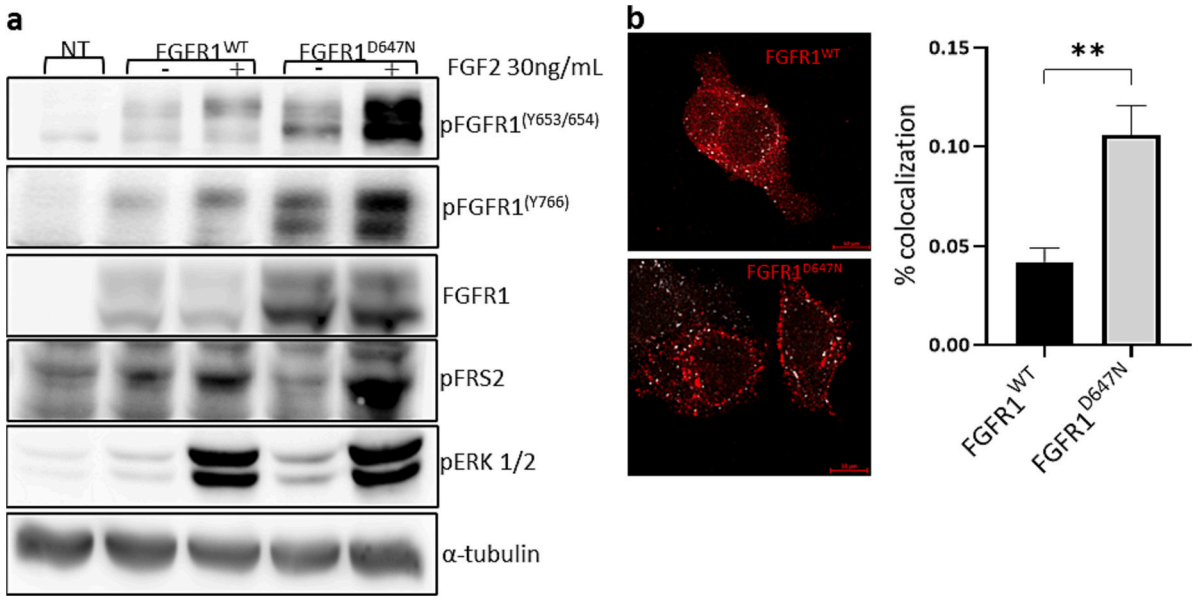

Fig. 2. FGFR1^{D647N} activates intracellular signaling in cancer cells. MCF7 were transfected with FGFR1^{WT} and FGFR1^{D647N}. a) WB analysis of pFGFR1(Y653/654), pFGFR1(Y766), total FGFR1, pFRS2, pAKT, pERK1/2 in the absence or in the presence of 30 ng/mL of FGF2. NT represents the non-transfected cells. Alpha-tubulin was used as a loading control. b) Immunofluorescence analysis for FGFR1 (red) and eea1 (white). FGFR1/eea1 colocalization was calculated by Zen software. (For interpretation of the references to colour in this figure legend, the reader is referred to the web version of this article.)

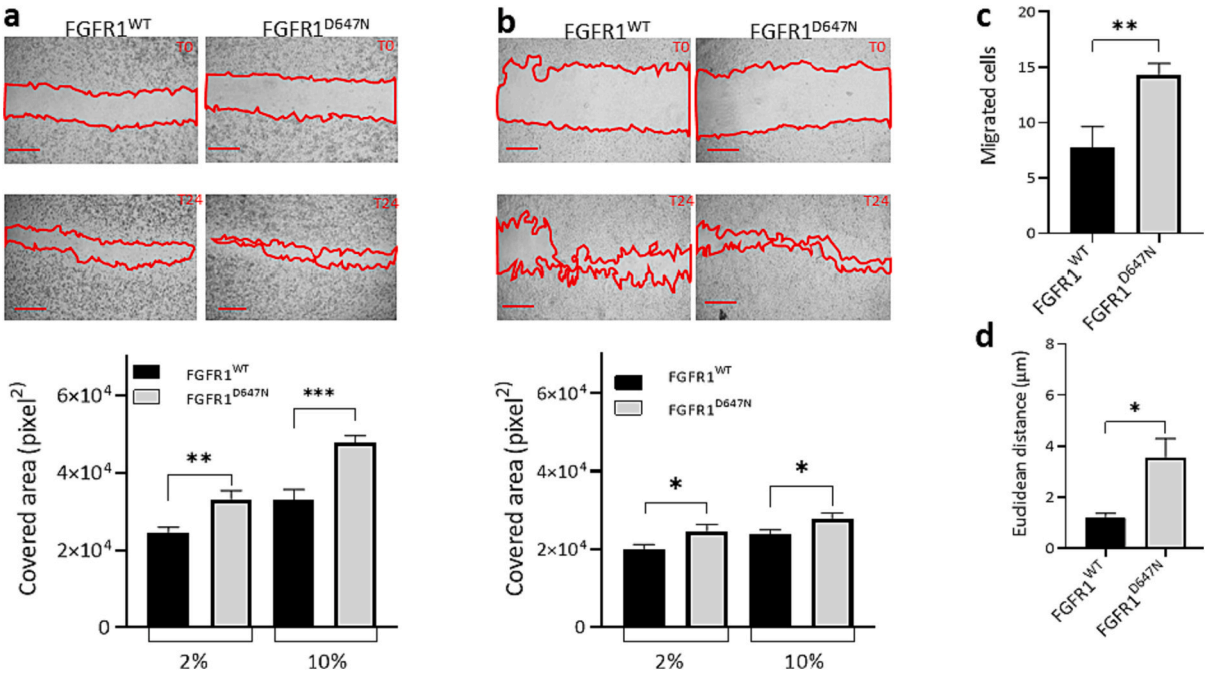

Fig. 3. FGFR1^{D647N} increases the migration capacity of human cancer cell lines. Scratch assay of A375 (a) and MCF7 (b) cells expressing FGFR1^{WT} or FGFR1^{D647N} receptors incubated in 2% or 10% FBS-containing medium. Representative images for cells incubated in 10% FBS are shown. Scratch areas before (upper image) and after 24-h incubation (lower image) are highlighted (red lines). Scale bar, 500 µm. Boyden chamber assay (c) or CAM migration assay (d) of A375-FGFR1^{WT} and A375-FGFR1^{D647N} cells. Data are shown as the mean ± SD of 3 independent transfections performed in triplicate. *, $p < 0.05$, **, $p < 0.01$, ***, p < 0,005, Student's *t*-Test. (For interpretation of the references to colour in this figure legend, the reader is referred to the web version of this article.)

FGFR1^{D647N} increases the motility of A375 cells, corroborating the pro-migratory effect of D647N substitution of FGFR1.

3.3. *FGFR1^{D647N} exacerbates the aggressiveness of cancer cells*

To evaluate the effect of FGFR1^{D647N} expression on the invasion ability, A375 spheroids were embedded in a fibrin gel in starving medium (0% FBS) or in basal medium (2% FBS). After 24 h, the invasion area was evaluated using ImageJ tool. As shown in Fig. 4a, FGFR1^{D647N}-A375 cells digest and invade the fibrin gel more efficiently than FGFR1^{WT}-A375 cells when maintained in basal medium supporting the hypothesis that the expression of mutant receptor confers a more malignant phenotype. Also, the expression of FGFR1^{D647N} increases the neoangiogenesis potential of A375 cells compared to FGFR1^{WT}, when

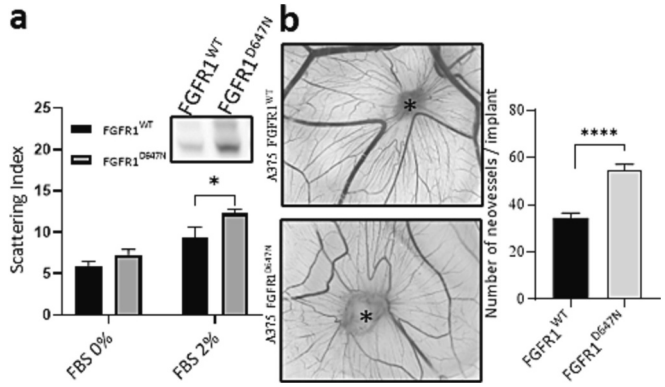

Fig. 4. The expression of FGFR1^{D647N} enhances the tumorigenic potential. a) Scattering index of A375-FGFR1^{WT} and A375-FGFR1^{D647N} cells in the presence of different stimuli: 0%, 2% and 10% FBS-containing medium. In the box WB of receptor expression; b) Representative images of neovessels converging through alginate pellet (*) containing A375-FGFR1^{WT} and A375-FGFR1^{D647N} cells onto CAM. Data are shown as the mean ± SEM of neovessels counted in 3 independent experiments ($n = 6$). *, $p < 0.05$, ****, p < 0,0001, Student's *t*-Test.

embedded in alginate pellets and engrafted onto the chicken chorioallantoic membrane (CAM) *in ovo* as shown by the significantly higher number of radial vessels (Fig. 4b). The more aggressive phenotype of FGFR1^{D647N}-A375 cells suggested that these cells produce proteolytic enzymes and soluble factors to support tumor progression and vascularization. These results corroborate the pronounced capacity of FGFR1^{D647N} of sustaining the acquisition of a more invasive/metastatic phenotype.

3.4. Mutated FGFR1^{D647N} shows increased sensitivity to the tyrosine kinase inhibitor erdafitinib

Besides altering tumor cell behavior, missense mutations within the A-loop of RTKs often affect their response to TKi. Here, we investigated whether the D647N substitution modifies the response of FGFR1 to erdafitinib, a clinically relevant pan-FGFR inhibitor approved by the FDA. FGFR1^{D647N} and FGFR1^{WT}-expressing HEK-293 T cells were treated with increasing doses of Erdafitinib and receptor phosphorylation was measured as a readout of kinase activity. Although in these experiments larger amounts of proteins were analyzed for FGFR1^{WT}-expressing HEK-293 T, in order to be able to clearly see the phosphorylation of the receptor, the results were normalized for the quantity of the receptor. All inhibitor doses were normalized with respect to the corresponding control excluding the possible effects due to different expression levels. Erdafitinib inhibits both FGFR1^{D647N} and FGFR1^{WT}, with a lower IC50 for FGFR1^{D647N} compared to FGFR1^{WT} (Fig. 5). Of note, Erdafitinib IC50 of FGFR1^{D647N} was similar to the one of FGF2-stimulated FGFR1^{WT} suggesting that the mutation induces conformational changes similar to that occurring in stimulated receptor.

To confirm the different sensitivity, we treated MCF7-FGFR1^{WT} and MCF7-FGFR1^{D647N} cells with IC10, IC50, and IC80 concentrations of erdafitinib for FGFR1^{WT} and FGFR1^{D647N} in a scratch assay. Results highlighted the expected reduction of cell motility (10, 50, and 80% respectively) in all experimental conditions confirming the erdafitinib sensitivity (Fig. 6).

4. Discussion

FGFR1 is a known oncogene and important therapeutic target in different types of cancer [17]. FGFR1 gene amplifications are common

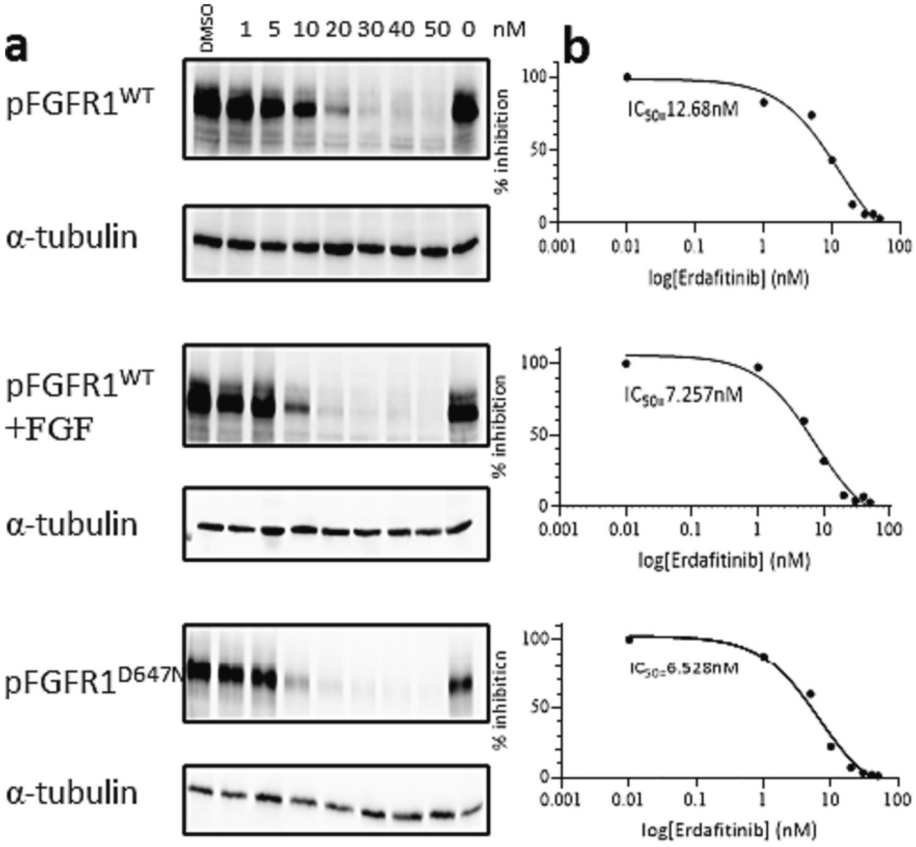

Fig. 5. Sensitivity of FGFR1^{D647N} to erdafitinib. HEK293T-FGFR1^{WT} and HEK293T-FGFR1^{D647N} cells were treated for 30 min with increasing concentrations of erdafitinib. a) Phosphorylation of -FGFR1^{WT}, FGF stimulated -FGFR1^{WT} and FGFR1^{D647N} and b) dose-inhibition curves. Alpha tubulin was used as a loaded control.

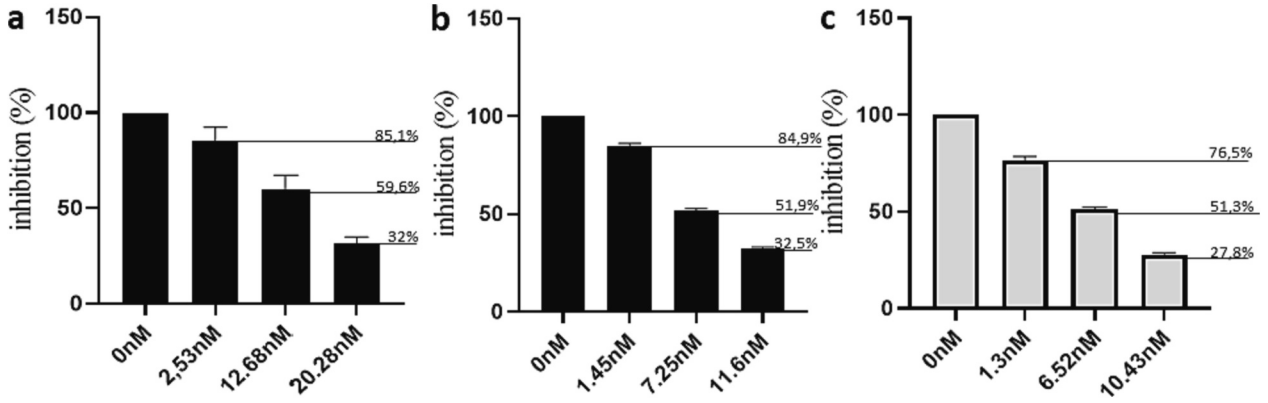

Fig. 6. Effects of erdafinitnib inhibition on cell migration. a) IC10, IC50 and IC80 concentrations of erdafitinib were used to treat MCF7- FGFR1^{WT} (a), FGF-stimulated MCF7-FGFR1^{WT} (b) and MCF7-FGFR1^{D647N}(c) cells in a scratch assay. Erdafitinib inhibition percentage was calculated. Data are shown as the mean ± SEM of 3 independent experiments.

in non-small cell lung carcinoma and hormone-receptor positive breast cancer where they are associated with poor prognosis and disease relapse. Missense point mutations of FGFR1 are also frequently detected in cancer with the substitutions N546K and K656E being the most frequent ones. Both these mutations increase receptor activity and cell transformation [18]. A variety of gene fusions involving FGFR1 gene have been also detected in multiple types of cancer. On these bases, different therapeutic approaches have been used to target FGFR1 alterations in cancer, including ligand traps, monoclonal antibodies and TKi [17]. In this context, a precise characterization of all FGFR1 alterations is critically needed for the effective application of FGFR1-targeted drugs, as these variants may be prognostically informative and could significantly alter drug sensitivity. Here we characterized the substitution D647N of FGFR1. D647 residue lies in the A-loop of the KD, a key regulatory region of the catalytic activity adjacent to the ATP-binding site. The phosphorylation of this region enhances the phosphoryl transfer rate of the kinase domain and increases its affinity for ATP [4]. Accordingly, FGFR1^{D647N} exhibits increased phosphorylation levels as compared to FGFR1^{WT} in the absence of exogenous FGF stimulation. However, ATP affinity remains in the same micromolar range for both receptors. In some KDs the A-loop acts as an auto-inhibitor, when unphosphorylated it collapses inside the protein, blocking the substrate binding [4]. We can speculate that substitution D647N affects the A-loop dynamic altering the ability of KD to interact with different substrates and drugs. Considering this, it is not surprising that D647N substitution leads a constitutive and ligand-independent receptor activation, and alters the tumor cells susceptibility to the FDA-approved pan-FGFR TKi Erdafitinib. [4]. Erdafitinib is a type 1.5 ATP-competitive inhibitor which binds to an inactive kinase with a DFG-in conformation. We can image that type1.5 inhibitors interact with their specific target during the transition from the inactive state with DFG-in to the active DFG-out conformation. Thus the D647N substitution may prevent the auto-inhibitor function favouring the DFG-out conformation. Of note, supporting this hypothesis, erdafitinib IC50 of FGFR1^{D647N} is similar to the one of FGF2-stimulated FGFR1^{WT}. Thus, the A-loop represents an interesting target to select specific ATP pocket binders as effective inhibitors and therapeutic choices. Overall, our results confirm that this mutation deserves further investigation as it may anticipate good response to given TKis in cancer patients.

The order of autophosphorylation of kinases is intrinsically controlled by the properties of the enzyme itself [4]. Recently it has been described that the order of autophosphorylation of FGFR1 (Y653, Y583, Y463, Y766, Y585, and Y654) is kinetically controlled and limited by the rate of phosphoryl transfer of the γ-phosphate group from ATP to the hydroxyl group of tyrosine [4]. *In vitro* studies suggested that the sequential order of phosphorylation may reflect different degrees of accessibility of the individual tyrosine sites within the three-dimensional structure of the FGFR1 KD. Although Y653 and Y583 show similar kinetics of phosphorylation, Y653 is phosphorylated at the very beginning to enhance the catalytic activity. Similarly, Y583 is phosphorylated long before Y585 [4]. D647N substitution leads to increased receptor phosphorylation at both Y653-Y654 and Y766. Thus, we speculate that this mutation may affect the tertiary structure of the KD altering the sequence of phosphorylation of tyrosine residues, which occurs also in the absence of FGF stimulation. This may temporally control the recruitment of downstream signaling molecules, explaining the altered activation of ERK 1/2 and FRS2 in FGFR1^{D647N}-expressing cells.

FGFR activation is well known for regulating cell motility and invasion under both physiological and pathological conditions [2]. In our experimental setup we investigated cell migration as a readout of FGFR1 activation. FGFR1^{D647N} expression in breast cancer and melanoma cells promotes both single cell and collective motility *in vitro* and *in vivo*, confirming that this mutation enhances pro-oncogenic effects.

The mutation D647N of FGFR1 occurs at position 256 of the KD, a mutational hotspot of the domain [18]. At this position, other known activating mutations occur, including R1051Q of VEGFR2, D1061N of FLT4, D650H of FGFR2, and the well-known oncogenic V600E mutation of B-Raf [7]. Remarkably, the B-Raf^{V600E} exhibits increased sensitivity to vemurafenib TKi, also belonging to type 1.5 TKis [19,20], similarly to erdafitinib. Despite this, many other mutations at this position remain uncharacterized. Therefore, the strength of our study is two fold: i) it corroborates the hypothesis that analogous mutations (detected at corresponding positions within a protein domain) in different proteins elicit similar effects; ii) it allows to transfer functional information for this mutation to other analogous ones in other kinases that have not been characterized yet. These results confirm that protein domain-based approaches enable to infer information for those variants that occur in small proportions of patients that cannot benefit from specific drugs. By doing so, they accelerate the characterization of all patient-specific alterations and might guide in the future the selection of drugs for a given patient, for a better application of precision oncology.

In conclusion, we have demonstrated that the newly identified D647N substitution of FGFR1 increases receptor activation, downstream signaling, migratory/oncogenic potential, and sensitivity to erdafitinib treatment. Despite being preliminary, our results confirm that position 256 of the KD is critical in regulating kinase function. Also this knowledge, which might become prognostically and/or therapeutically significant, can be transferred to additional uncharacterized mutations occurring at position 256 of the kinase domain of other cancer-associated kinases.

CRediT authorship contribution statement

Mattia Domenichini: Conceptualization, Formal analysis, Data curation, Investigation, Writing – review & editing, Writing – original draft. **Cosetta Ravelli:** Investigation. **Michela Corsini:** Investigation. **Silvia Codenotti:** Investigation. **Elisa Moreschi:** Investigation. **Daniela Zizioli:** Investigation. **Roberto Bresciani:** Investigation. **Elisabetta Grillo:** Conceptualization, Formal analysis, Data curation, Investigation, Writing – review & editing, Writing – original draft. **Stefania Mitola:** Conceptualization, Formal analysis, Data curation, Writing – review & editing, Writing – original draft, Project administration.

Declaration of Competing Interest

The authors declare the following financial interests/personal relationships which may be considered as potential competing interests:

Mitola Stefania and Michela Corsini reports financial support was provided by Italian Association for Cancer Research. Silvia Codenotti and Elisabetta Grillo reports financial support was provided by Umberto Veronesi Foundation.

Data availability

No data was used for the research described in the article.

Acknowledgments

This work was supported by grants from Associazione Italiana per la Ricerca sul Cancro (AIRC) to S.M. (IG 2021 Id 25726). *E.G.* and S.C. were supported by Fondazione Umberto Veronesi (FUV) and M.C. by AIRC (ID 26917-2021) fellowships.

Declaration of generative AI in scientific writing

We declare that no AI-assisted technologies were applied in the writing process of this manuscript.

Appendix A. Supplementary data

Supplementary data to this article can be found online at https://doi.org/10.1016/j.bbagen.2023.130470.

References

[1] S. Sarabipour, K. Hristova, Mechanism of FGF receptor dimerization and activation, Nat. Commun. 7 (1) (2016) 10262, https://doi.org/10.1038/ncomms10262.
[2] R. Porta, R. Borea, A. Coelho, S. Khan, A. Araújo, P. Reclusa, T. Franchina, N. Van Der Steen, P. Van Dam, J. Ferri, R. Sirera, A. Naing, D. Hong, C. Rolfo, FGFR a promising druggable target in cancer: molecular biology and new drugs, Crit. Rev. Oncol. Hematol. 113 (2017) 256–267, https://doi.org/10.1016/j.critrevonc.2017.02.018.
[3] K.C. Hart, S.C. Robertson, M.Y. Kanemitsu, A.N. Meyer, J.A. Tynan, D.J. Donoghue, Transformation and stat activation by derivatives of FGFR1, FGFR3, and FGFR4, Oncogene 19 (29) (2000) 3309–3320, https://doi.org/10.1038/sj.onc.1203650.
[4] E.D. Lew, C.M. Furdui, K.S. Anderson, J. Schlessinger, The precise sequence of FGF receptor autophosphorylation is kinetically driven and is disrupted by oncogenic mutations, Sci. Signal. 2 (58) (2009) ra6, https://doi.org/10.1126/scisignal.2000021.
[5] E. Grillo, C. Ravelli, M. Corsini, C. Gaudenzi, L. Zammataro, S. Mitola, Novel potential oncogenic and druggable mutations of FGFRs recur in the kinase domain across cancer types, Biochim. Biophys. Acta (BBA) - Mol. Basis Dis. 2022 (2) (1868) 166313, https://doi.org/10.1016/j.bbadis.2021.166313.
[6] G.E.M. Melloni, S. de Pretis, L. Riva, M. Pelizzola, A. Céol, J. Costanza, H. Müller, L. Zammataro, LowMACA: exploiting protein family analysis for the identification of rare driver mutations in cancer, BMC Bioinforma. 17 (1) (2016) 80, https://doi.org/10.1186/s12859-016-0935-7.
[7] E. Grillo, C. Ravelli, M. Corsini, L. Zammataro, S. Mitola, Protein domain-based approaches for the identification and prioritization of therapeutically actionable cancer variants, Biochim. Biophys. Acta (BBA) - Rev. Cancer 2021 (2) (1876) 188614, https://doi.org/10.1016/j.bbcan.2021.188614.
[8] R. Nussinov, H. Jang, A. Gursoy, O. Keskin, V. Gaponenko, Inhibition of nonfunctional Ras, Cell Chem. Biol. 28 (2) (2021) 121–133, https://doi.org/10.1016/j.chembiol.2020.12.012.
[9] R. Roskoski, Classification of small molecule protein kinase inhibitors based upon the structures of their drug-enzyme complexes, Pharmacol. Res. 103 (2016) 26–48, https://doi.org/10.1016/j.phrs.2015.10.021.
[10] M. Teng, M.R. Luskin, S.W. Cowan-Jacob, Q. Ding, D. Fabbro, N.S. Gray, The Dawn of allosteric BCR-ABL1 drugs: from a phenotypic screening hit to an approved drug, J. Med. Chem. 65 (11) (2022) 7581–7594, https://doi.org/10.1021/acs.jmedchem.2c00373.
[11] S. Chung, T. Andersson, K.C. Sonntag, L. Björklund, O. Isacson, K.S. Kim, Analysis of different promoter systems for efficient transgene expression in mouse embryonic stem cell lines, Stem Cells 20 (2) (2002) 139–145, https://doi.org/10.1634/stemcells.20-2-139.
[12] D. Leali, R. Bianchi, A. Bugatti, S. Nicoli, S. Mitola, L. Ragona, S. Tomaselli, G. Gallo, S. Catello, V. Rivieccio, L. Zetta, M. Presta, Fibroblast growth factor 2-antagonist activity of a long-pentraxin 3-derived anti-angiogenic pentapeptide, J. Cell. Mol. Med. 14 (8) (2010) 2109–2121, https://doi.org/10.1111/j.1582-4934.2009.00855.x.
[13] E.C. Hulme, M.A. Trevethick, Ligand binding assays at equilibrium: validation and interpretation, Br. J. Pharmacol. 161 (6) (2010) 1219–1237, https://doi.org/10.1111/j.1476-5381.2009.00604.x.
[14] F. Maule, S. Bresolin, E. Rampazzo, D. Boso, A. Della Puppa, G. Esposito, E. Porcù, S. Mitola, G. Lombardi, B. Accordi, M. Tumino, G. Basso, L. Persano, Annexin 2A sustains glioblastoma cell dissemination and proliferation, Oncotarget 7 (34) (2016) 54632–54649, https://doi.org/10.18632/oncotarget.10565.
[15] E. Siraliev-Perez, J.T.B. Stariha, R.M. Hoffmann, B.R.S. Temple, Q. Zhang, N. Hajicek, M.L. Jenkins, J.E. Burke, J. Sondek, Dynamics of allosteric regulation of the phospholipase C-γ isozymes upon recruitment to membranes, Elife 11 (2022), https://doi.org/10.7554/eLife.77809.
[16] M.A. Krook, J.W. Reeser, G. Ernst, H. Barker, M. Wilberding, G. Li, H.Z. Chen, S. Roychowdhury, Fibroblast growth factor receptors in cancer: genetic alterations, diagnostics, therapeutic targets and mechanisms of resistance, Br. J. Cancer 124 (5) (2021) 880–892, https://doi.org/10.1038/s41416-020-01157-0.
[17] F. Cimmino, A. Montella, M. Tirelli, M. Avitabile, V.A. Lasorsa, F. Visconte, S. Cantalupo, T. Maiorino, B. De Angelis, M. Morini, A. Castellano, F. Locatelli, M. Capasso, A. Iolascon, FGFR1 is a potential therapeutic target in neuroblastoma, Cancer Cell Int. 22 (1) (2022) 174, https://doi.org/10.1186/s12935-022-02587-x.
[18] E. Grillo, M. Corsini, C. Ravelli, M. di Somma, L. Zammataro, E. Monti, M. Presta, S. Mitola, A novel variant of VEGFR2 identified by a pan-cancer screening of recurrent somatic mutations in the catalytic domain of tyrosine kinase receptors enhances tumor growth and metastasis, Cancer Lett. 496 (2021) 84–92, https://doi.org/10.1016/j.canlet.2020.09.027.
[19] D. Fabbro, S.W. Cowan-Jacob, H. Moebitz, Ten things you should know about protein kinases: IUPHAR review 14, Br. J. Pharmacol. 172 (11) (2015) 2675–2700, https://doi.org/10.1111/bph.13096.
[20] P.B. Chapman, A. Hauschild, C. Robert, J.B. Haanen, P. Ascierto, J. Larkin, R. Dummer, C. Garbe, A. Testori, M. Maio, D. Hogg, P. Lorigan, C. Lebbe, T. Jouary, D. Schadendorf, A. Ribas, S.J. O'Day, J.A. Sosman, J.M. Kirkwood, A. M. Eggermont, B. Dreno, K. Nolop, J. Li, B. Nelson, J. Hou, R.J. Lee, K.T. Flaherty, G.A. McArthur, Improved survival with vemurafenib in melanoma with BRAF V600E mutation, N. Engl. J. Med. 364 (26) (2011) 2507–2516, https://doi.org/10.1056/NEJMoa1103782.